On making nD images well-composed by a self-dual local interpolation

Nicolas Boutry[1,2], Thierry Géraud[1], and Laurent Najman[2]

[1] EPITA Research and Development Laboratory (LRDE)
[2] Université Paris-Est, LIGM, Équipe A3SI, ESIEE
firstname.lastname@lrde.epita.fr, l.najman@esiee.fr

Abstract. Natural and synthetic discrete images are generally not well-composed, what leads to many topological issues : the connectivities in binary images are not equivalent, the Jordan Separation theorem is not true anymore, and so on. At the converse, making images well-composed solves those problems and then gives access to many powerful tools already known in mathematical morphology as the Tree of Shapes which is of our principal interest. So in this paper, we present two main results: the characterization of 3D well-composed gray-valued images and a counter-example showing that no usual local self-dual interpolation makes well-composed images with one subdivision in 3D as soon as we choose the mean operator to interpolate in 1D. Then, we briefly discuss the various constraints it could be interesting to change to make the problem solvable in nD.

Keywords: Digital topology, gray-level images, well-composed sets, well-composed images

1 Introduction

Natural and synthetic images are usually not well-composed, that leads to many topological issues. As an example, the Jordan Separation theorem, stating that a simple closed curve in $\mathbb{R}^2$ separates the space in only two components is not true anymore in binary 2D discrete images [5]. To solve this problem, we have to juggle with two complementary connectivities: 4 for the background and 8 for the foreground, or the inverse, while well-composed binary images have the fundamental property to make the 4- and 8-connectivities equivalent, and then this topological issue vanishes. In the same manner, well-composed nD images, with $n > 2$, make $2n$- and $(3^n - 1)$-connectivities equivalent [10]. Other advantages appear with well-composed images like the preservation of the topological properties by a rigid transformation [9], the simplification of thinning algorithms [7] and of the resulting graph structures of the skeletons [5]. Also, and it is our most important goal, making an image well-composed allows to compute its tree of shapes [8,2] with a quasi-linear algorithm that can be found in [3]. An introduction to the three of shapes in the continuous case can be found in [1]. In the same manner, not to favorize bright components on dark background or dark

components over bright background or the converse, like for the biomedical images, the process to make images well-composed has to be self-dual, and because we do not want to deteriorate the initial signal, we use an interpolation method.

Section 2 recalls the definitions of 2D and 3D well-composed sets and gray-valued images, and introduces a characterization of 3D gray-valued well-composed images. We present in Section 3 the general scheme that defines recursively usual ordered local in-between interpolation methods with one subdivision. We also show that this restrictive scheme applied to self-dual methods imply that this kind of interpolation methods fail in 3D (and then further) to make well-composed images. We conclude in Section 4 with some perspectives that could work in nD even if $n > 2$ (in a local and a non-local ways).

2 A characterization of 3D well-composed gray-valued images

2.1 2D WC Sets and Gray-Valued Images

Let us begin by the definitions of a block of $\mathbb{Z}^n$, so we will be able to recall the definition and the characterization of 2D well-composed sets and images.

A block in nD associated to $z \in \mathbb{Z}^n$ is the set S_z defined such that $S_z = \left\{ z' \in \mathbb{Z}^n \middle| ||z - z'||_\infty \leq 1 \text{ and } \forall i \in [1, n], z'_i \geq z_i \right\}$. Moreover, we call blocks of $\mathcal{D} \subseteq \mathbb{Z}^n$ any element of the set $\left\{ S_z \middle| \exists z \in \mathcal{D}, S_z \subseteq \mathcal{D} \right\}$.

Definition 1 (2D WC Sets [5]) *A set X is weakly well-composed if any 8-component of X is a 4-component. X is well-composed if both X and its complement $X^c = \mathbb{Z}^2 \setminus X$ are weakly well-composed.*

Proposition 1 (Local Connectivity and No Critical Configurations [5]) *A set $X \subseteq \mathbb{Z}^2$ is well-composed iff it is locally 4-connected. Also, a set X is well-composed if none of the critical configurations $\begin{pmatrix} 1 & 0 \\ 0 & 1 \end{pmatrix}$ or $\begin{pmatrix} 0 & 1 \\ 1 & 0 \end{pmatrix}$ appears in X.*

Definition 2 (Cuts in nD) *For any $\lambda \in \mathbb{R}$ and any gray-valued map $u : \mathcal{D} \subseteq \mathbb{Z}^n \mapsto \mathbb{R}$, we denote by $[u > \lambda]$ and $[u < \lambda]$ the sets $[u > \lambda] = \left\{ M \in \mathcal{D} \middle| u(M) > \lambda \right\}$ and $[u < \lambda] = \left\{ M \in \mathcal{D} \middle| u(M) < \lambda \right\}$. We call them respectively upper strict cuts and lower strict cuts [3].*

We will note that an image $u : \mathcal{D} \subseteq \mathbb{Z}^2 \mapsto \mathbb{R}$ cannot be well-composed if its domain $\mathcal{D}$ is finite and not well-composed (since $[u < \max(u) + 1] = \mathcal{D}$).

Definition 3 (Gray-valued WC 2D Maps [5]) *A gray-level map u is* well-composed *iff for every $\lambda \in \mathbb{R}$, the strict cuts $[u > \lambda]$ and $[u < \lambda]$ result in well-composed sets.*

We recall that the *interval value* of the couple $(x, y) \in \mathbb{R}^2$ is defined as $\text{intvl}(x, y) = [\min(x, y), \max(x, y)]$.

Proposition 2 (Characterization of 2D WC maps [5]) *A gray-level image is well-composed iff for every 2D block S such that $u\big|_S = \begin{pmatrix} a & b \\ c & d \end{pmatrix}$, the interval values satisfy* $\mathrm{intvl}(a,d) \cap \mathrm{intvl}(b,c) \neq \emptyset$.

2.2 3D WC Sets and Gray-Valued Maps

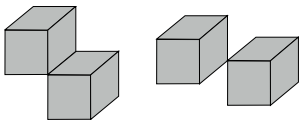

Fig. 1. Illustration of the bdCA of a set containing a critical configurations of type 1 (left), and of type 2 (right).

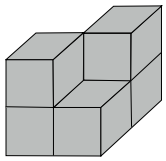

Fig. 2. A set locally 6-connected but not well-composed.

As we will see, for $n = 3$ we loose the equivalence between the local connectivity and the well-composedness, and for this reason Latecki introduced the continuous analog.

Definition 4 (CA and bdCA [4]) *The* continuous analog $\mathrm{CA}(z)$ *of a point $z \in \mathbb{Z}^3$ is the closed unit cube centered at this point with faces parallel to the coordinate planes, and the continuous analog of a set $X \subseteq \mathbb{Z}^3$ is defined as* $\mathrm{CA}(X) = \bigcup \{\mathrm{CA}(x) | x \, in X\}$. *The (face) boundary of the continuous analog* $\mathrm{CA}(X)$ *of a set $X \subseteq \mathbb{Z}^3$ is noted* $\mathrm{bdCA}(X)$ *and defined as the union of the set of closed faces each of which is the common face of a cube in* $\mathrm{CA}(X)$ *and a cube not in* $\mathrm{CA}(X)$.

Definition 5 (Well-composedness in 3D [4]) *A 3D set $X \subseteq \mathbb{Z}^3$ is well-composed iff* $\mathrm{bdCA}(X)$ *is a 2D manifold, i.e., a topological space which is locally Euclidian.*

Proposition 3 (No Critical Configurations [4]) *A set $X \subseteq \mathbb{Z}^3$ is well-composed iff the following critical configurations of cubes of type 1 or of type 2 (modulo reflections and rotations) do not occur in* $\mathrm{CA}(X)$ *or in* $CA(X^c)$ *(see Figure 1).*

One can remark that if a set $X \subseteq \mathbb{Z}^3$ is well-composed, then X is locally 6-connected, but the opposite is not true (see Figure 2).

Definition 6 (WC Gray-valued Maps) *We say that a 3D real-valued map $u : \mathcal{D} \subseteq \mathbb{Z}^3 \mapsto \mathbb{R}$ is well-composed if its strict cuts $[u > \lambda]$ and $[u < \lambda]$, $\forall \lambda \in \mathbb{R}$, are well-composed.*

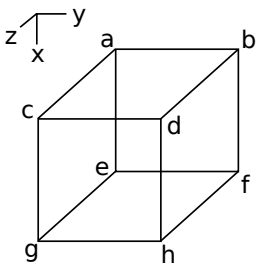

Fig. 3. The restriction $u\big|_S$ of u to a 3D block S.

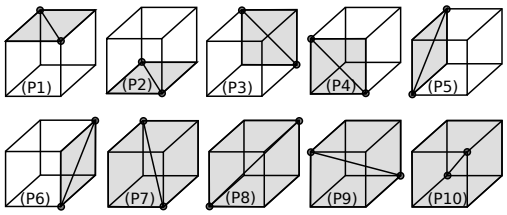

Fig. 4. The ten characteristical relations of well-composedness of a gray-valued image u restricted to a 3D block S.

To characterize 3D gray-level well-composed images, we first give two lemmas concerning the detection of the critical configurations of respectively type 1 and type 2.

Lemma 1 *The strict cuts* $[u > \lambda]$ *and* $[u < \lambda]$, $\lambda \in \mathbb{R}$, *of a gray-valued image* u *defined on a block* S, *such as depicted in Figure 3, do not contain any critical configuration of type 1 iff the six following properties hold:*

$\text{intvl}(a,d) \bigcap \text{intvl}(b,c) \neq \emptyset$ $(P1)$, $\quad \text{intvl}(e,h) \bigcap \text{intvl}(g,f) \neq \emptyset$ $(P2)$

$\text{intvl}(a,f) \bigcap \text{intvl}(b,e) \neq \emptyset$ $(P3)$, $\quad \text{intvl}(c,h) \bigcap \text{intvl}(g,d) \neq \emptyset$ $(P4)$

$\text{intvl}(a,g) \bigcap \text{intvl}(e,c) \neq \emptyset$ $(P5)$, $\quad \text{intvl}(b,h) \bigcap \text{intvl}(f,d) \neq \emptyset$ $(P6)$

Proof : Let us assume that any of these properties $(P_i), i \in [1,6]$, is false. Let us say it is the case of $(P1)$. Then two cases are possible: either $\max(a,d) < \min(b,c)$, and that means that there exists $\lambda = (\max(a,d) + \min(b,c))/2$ such that $[u < \lambda]$ contains the critical configuration of type 1 $\{a,d\}$, or $\min(a,d) > \max(b,c)$, and there exists $\lambda = (\min(a,d) + \max(b,c))/2$ such that one more time $[u > \lambda]$ contains the critical configuration of type 1 $\{a,d\}$. The reasoning is the same for all the other properties. Conversely, let us assume that there exists $\lambda \in \mathbb{R}$ such that either $[u > \lambda]$ or $[u < \lambda]$ contains a critical configuration of type 1. That means immediately that one of the 6 properties $P_i, i \in [1,6]$, corresponding to each of the six faces of the block S, is false (see Figure 4 for the faces concerned by the properties).

Let us recall that the span of a set of values $E \subseteq \mathbb{R}$ is $\text{span}(E) = [\inf(E), \sup(E)]$.

Lemma 2 *The strict cuts* $[u > \lambda]$ *and* $[u < \lambda]$, $\lambda \in \mathbb{R}$, *of a gray-valued image* u *defined on a block* S *such as depicted in Figure 3, do not contain any critical configuration of type 2 iff the four following properties are true:*

$\text{intvl}(a,h) \bigcap \text{span}\{b,c,d,e,f,g\} \neq \emptyset$ $(P7)$

$\text{intvl}(b,g) \bigcap \text{span}\{a,c,d,e,f,h\} \neq \emptyset$ $(P8)$

$\text{intvl}(c,f) \bigcap \text{span}\{a,b,d,e,g,h\} \neq \emptyset$ $(P9)$

$\text{intvl}(d,e) \bigcap \text{span}\{a,b,c,f,g,h\} \neq \emptyset$ $(P10)$

Proof : Let us assume that any of these properties $(P_i), i \in [7,10]$, is false. Let us say it is the case of $(P7)$. Then two cases are possible: either $\max(a,h) <$

$\min(b,c,d,e,f,g)$, and that means that there exists $\lambda = (\max(a,h)+\min(b,c,d,e,f,g))/2$ such that $[u < \lambda]$ contains the critical configuration of type 2 $\{a,h\}$, or $\min(a,h) > \max(b,c,d,e,f,g)$, and there exists $\lambda = (\min(a,h) + \max(b,c,d,e,f,g))/2$ such that one more time $[u > \lambda]$ contains the critical configuration of type 2 $\{a,h\}$. The reasoning is the same for all the other properties. Conversely, let us assume that there exists $\lambda \in \mathbb{R}$ such that either $[u > \lambda]$ or $[u < \lambda]$ contains a critical configuration of type 2. That means immediately that one of the 4 properties $P_i, i \in [7,10]$, corresponding to each of the four diagonals of the block S, is false (see Figure 4).

We are know ready to the main theorem of this section, characterizing the well-composedness on a 3D gray-valued image.

Theorem 1 (Characterization of well-composedness in 3D) *Let us suppose that $\mathcal{D}$ is an hyperrectangle in $\mathbb{Z}^3$. A gray-valued 3D image $u : \mathcal{D} \mapsto \mathbb{R}$ is well-composed on $\mathcal{D}$ iff on any block $S \subseteq \mathcal{D}$, $u\big|_S$ satisfies the properties $(P_i), i \in [1,10]$.*

3 Local interpolation Methods

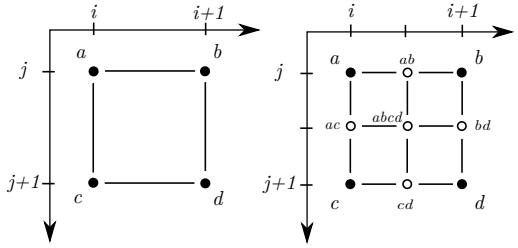

Fig. 5. Illustration of the subdivision process on a block S.

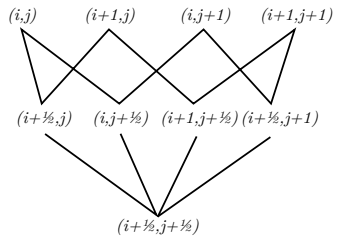

Fig. 6. $s(S) \subseteq \left(\frac{\mathbb{Z}}{2}\right)^n$ as a poset.

Using interpolation methods with one subdivision does not deteriorate the initial signal. The size of the original image is multiplied by a factor of 2^n, where n is the dimension of the space of the image. Figure 5 illustrates this subdivision process.

3.1 Subdivision of a Domain and $\left(\frac{\mathbb{Z}}{2}\right)^n$ as a poset

Let us introduce the subdivision of a block that allows us to provide an order on the elements. Using this order, the subdivided space is a poset.

Let z be a point in $\mathbb{Z}^n$, and S_z its associated block. Then we define the subdivision of S_z as $s(S_z) = \{z' \in \left(\frac{\mathbb{Z}}{2}\right)^n \big| ||z - z'||_\infty \leq 1 \text{ and } \forall i \in [1,n], z'_i \geq$

$z_i\}$. Then, we define the subdivision of a domain $\mathcal{D} \subseteq \mathbb{Z}^n$ as the union of the subdivisions of the blocks contained in $\mathcal{D}$, i.e., $s(\mathcal{D}) = \bigcup_{S \subseteq \mathcal{D}} s(S)$.

Definition 7 (Order of a point of $\left(\frac{\mathbb{Z}}{2}\right)^n$) *Assume e_i is a fixed basis of $\mathbb{Z}^n$. We note $\frac{1}{2}(z) = \{i \in [1,n] \big| z_i \in \frac{\mathbb{Z}}{2} \setminus \mathbb{Z}\}$ (where z_i represents the i^{th} coordinate of z). The sets $\mathbb{E}_k$ for $k \in [0,n]$, are defined such that $\mathbb{E}_k = \{z \in \left(\frac{\mathbb{Z}}{2}\right)^n \ \big| \ \big|\frac{1}{2}(z)\big| = k\}$ (where $\big|E\big|$ denotes the cardinal of the set E), and represent a partition of $\left(\frac{\mathbb{Z}}{2}\right)^n$. We call* order *of a point z the value k such that $z \in \mathbb{E}_k$ and we note it $\mathfrak{o}(z)$.*

Definition 8 (Parents in $\left(\frac{\mathbb{Z}}{2}\right)^n$) *Let z be a point of $\left(\frac{\mathbb{Z}}{2}\right)^n$. The set of the* parents *of $z \in \left(\frac{\mathbb{Z}}{2}\right)^n$, noted $\mathbb{P}(z)$, is defined by $\mathbb{P}(z) = \cup_{i \in \frac{1}{2}(z)} \{z - \frac{e_i}{2}, z + \frac{e_i}{2}\}$. The parents of $z \in \left(\frac{\mathbb{Z}}{2}\right)^n$ of order 0 are $\mathbb{P}^0(z) = \{z\}$ and of order $k > 0$ are defined recursively by $\mathbb{P}^k(z) = \mathbb{P}^{k-1}(\mathbb{P}(z))$.*

Definition 9 ($\mathcal{G}(z)$ and $\mathbb{A}(z)$) *Let z be a point of $\left(\frac{\mathbb{Z}}{2}\right)^n$. We define the set $\mathcal{G}(z) = \cup_{k \in [0, \mathfrak{o}(z)]} \mathbb{P}^k(z)$. The* ancesters *of $z \in \left(\frac{\mathbb{Z}}{2}\right)^n$ are $\mathbb{A}(z) = \mathbb{P}^{\mathfrak{o}(z)}(z)$.*

Notice that $\mathbb{A}(z) \subseteq \mathbb{Z}^n$ and that any point $z \in \mathbb{E}_k$, $k \in [1,n]$, has its parents in $\mathbb{E}_{k-1}$. Hence $\{\mathbb{E}_k\}_{k \in [0,n]}$ is a (hierarchical) partition of $\left(\frac{\mathbb{Z}}{2}\right)^n$, so $\left(\left(\frac{\mathbb{Z}}{2}\right)^n, \mathbb{P}\right)$ is a poset (see Figure 6).

Definition 10 (Opposites) *Let z be a point of $\left(\frac{\mathbb{Z}}{2}\right)^n$. The* opposites *of $z \in \left(\frac{\mathbb{Z}}{2}\right)^n$, noted* $\mathrm{opp}(z)$*, is the family of pairs of points such that* $\mathrm{opp}(z) = \cup_{i \in \frac{1}{2}(z)} \big\{\{z - \frac{e_i}{2}, z + \frac{e_i}{2}\}\big\}$.

3.2 Interpolation methods with one subdivision

Let us recall that the convex hull $\mathrm{convhull}(Z)$ of a set of m points $Z = \{z^1, \ldots, z^m\} \subseteq \mathbb{Z}^n$ is:

$$\mathrm{convhull}(Z) = \left\{ \sum_{i=1}^{m} \alpha_i z^i \ \Big| \ \sum_{i=1}^{m} \alpha_i = 1 \text{ and } \forall i \in [1,m], \alpha_i \geq 0 \right\}$$

Definition 11 (Subdivision of edges, faces, and cubes) *Let $\mathcal{E} = \{z_1, z_2\}$ be an edge in $\mathbb{Z}^n$. The subdivision of $\mathcal{E}$ is $s(\mathcal{E}) = \{z \in \left(\frac{\mathbb{Z}}{2}\right)^n \big| z \in \mathrm{convhull}(\mathcal{E})\}$. The subdivision of a face $\mathcal{F} = \{z_1, z_2, z_3, z_4\}$ is $s(\mathcal{F}) = \{z \in \left(\frac{\mathbb{Z}}{2}\right)^n \big| z \in \mathrm{convhull}(\mathcal{F})\}$. The subdivision of a cube $\mathcal{C} = \{z_1, \ldots, z_8\}$ is $s(\mathcal{C}) = \{z \in \left(\frac{\mathbb{Z}}{2}\right)^n \big| z \in \mathrm{convhull}(\mathcal{C})\}$.*

3.3 The set of properties that the interpolation method has to satisfy

The *interpolation* of a map $u : \mathcal{D} \subseteq \mathbb{Z}^n \mapsto \mathbb{R}$ to a map $\mathfrak{I}(u) : s(\mathcal{D}) \subseteq \left(\frac{\mathbb{Z}}{2}\right)^n \mapsto \mathbb{R}$ is a transformation such that $\mathfrak{I}(u)\big|_S = u\big|_S$ for any block $S \subseteq \mathcal{D}$.

Let $u : \mathcal{D} \subseteq \mathbb{Z}^3 \mapsto \mathbb{R}$ be any 3D gray-valued image. We say that an interpolation method $\mathfrak{I} : u \mapsto \mathfrak{I}(u)$ is *self-dual* iff $\mathfrak{I}(-u) = -\mathfrak{I}(u)$. The main interest in the self-duality is that the interpolation method does not overemphasizes bright components at the expense of the dark ones or the inverse.

An interpolation method $\mathfrak{I} : u \mapsto \mathfrak{I}(u)$ in 3D is said *ordered* if the new values are inserted firstly at the centers of the subdivided edges, secondly at the centers of the subdivided faces, and finally at the center of the subdivided cube.

An ordered interpolation method is said *in between* iff it puts the values at a point z in between the values of its parents $\mathbb{P}(z)$.

Finally, we say that an interpolation method is *well-composed* iff the image $\mathfrak{I}(u)$ resulting from the interpolation of u is well-composed for any given image u.

So there is the set of properties that the interpolation method we are interested in has to verify:

$$(\mathcal{P}) \Leftrightarrow \begin{cases} \mathfrak{I} \text{ is invariant by translations, } \frac{\pi}{2}\text{'s rotations and axial symmetries} \\ \mathfrak{I} \text{ is ordered} \\ \mathfrak{I} \text{ is in-between} \\ \mathfrak{I} \text{ is self-dual} \\ \mathfrak{I} \text{ is well-composed} \end{cases}$$

3.4 The scheme of local interpolation methods verifying $\mathcal{P}$

A *local interpolation* $\mathfrak{I}$ is an interpolation such as for any block $S \subseteq \mathcal{D}$, $\mathfrak{I}(u)$ on $s(S)$ is computed only from its nearest neighbours belonging to $\mathbb{E}_0$ (we see an image as a graph). For convenience, we will write u' instead of $\mathfrak{I}(u)$ for local interpolation methods in the sequel.

Lemma 3 (The scheme for local interpolation methods) *Any local interpolation method $\mathfrak{I}$ on $\left(\frac{\mathbb{Z}}{2}\right)^n$ verifying $\mathcal{P}$ can be characterized by a set of functions $\{f_k\}_{k\in[1,n]}$ such that:*

$$\forall\, z \in \left(\frac{\mathbb{Z}}{2}\right)^n,\ u'(z) = \begin{cases} u(z) & \text{if } z \in \mathbb{E}_0 \\ f_k(u|_{\mathbb{A}(z)}) & \text{if } z \in \mathbb{E}_k,\ k \in [1,n] \end{cases}$$

We denote such an interpolation method $\mathfrak{I}_{f_1,\ldots,f_n}$.

Proof : Because the interpolation process on the subdivided edges depends only on the values of u at the vertices of the original edges due to the locality of the method, and because it has to be invariant by axial symmetries and rotations, there is an unique function f_1 characterizing the interpolation method on the subdivided edges. The reasoning is the same on the faces and the cube respectively for f_2 and f_3.

Notice that it is an implication and not an equivalence: an interpolation method verifying this scheme does not verify all the properties in $\mathcal{P}$.

3.5 I_0, I_{WC}, and I_{sol} for local interpolation methods

Let us introduce some useful sets to express recursively the local interpolation methods satisfying the properties $\mathcal{P}$ we are looking for.

Definition 12 (I_0 and definition of a local in-between interpolation method) *Let $u : \mathcal{D} \mapsto \mathbb{R}$ be a gray-valued map, let z be a point of $s(\mathcal{D}) \setminus \mathbb{E}_0$, and let $\mathfrak{I}$ be a given local interpolation method. We define the set $I_0(u, z)$ associated to $\mathfrak{I}$ by:*

$$I_0(u,z) \overset{(def)}{=} \bigcap_{\{z^-,z^+\}\in \mathrm{opp}(z)} \mathrm{intvl}(u'(z^-), u'(z^+))$$

Then, an ordered local interpolation method $\mathfrak{I}$ is said in-between iff $u'(z) \in I_0(u, z)$ for any image $u : \mathcal{D} \mapsto \mathbb{R}$ and $z \in s(\mathcal{D}) \setminus \mathbb{E}_0$.

Definition 13 (I_{WC} and I_{sol}) *Let $u : \mathcal{D} \mapsto \mathbb{R}$ be a gray-valued image, z be a point of $s(\mathcal{D}) \setminus \mathbb{E}_0$, and $\mathfrak{I}$ be a given local interpolation method. We define the set $I_{WC}(u, z)$ associated to $\mathfrak{I}$ such as for any $z \in \mathbb{E}_1$, $I_{WC}(u, z) = \mathbb{R}$ and for any $z \in \mathbb{E}_k$ with $k \geq 2$:*

$$I_{WC}(u,z) \;=\; \{\, v \in \mathbb{R} \;\mid\; u'(z) = v \;\Rightarrow\; u'\big|_{\mathcal{G}(z)} \text{ is well-composed} \,\}$$

Last, let us denote $I_{sol}(u, z) = I_0(u, z) \cap I_{WC}(u, z)$.

Then we obtain the following scheme, necessary (but not sufficient) to satisfy $\mathcal{P}$.

Theorem 2 *Any local interpolation $\mathfrak{I}$ method satisfying $\mathcal{P}$ is such that:*
$\forall z \in \left(\frac{\mathbb{Z}}{2}\right)^n, u'(z) = \begin{cases} u(z) & \text{if } z \in \mathbb{E}_0 \\ f_k(u\big|_{\mathbb{A}(z)}) \in I_{sol}(u,z) & \text{if } z \in \mathbb{E}_k, k \in [1,n] \end{cases}$

Notice that such a local interpolation method $\mathfrak{I}$ is ordered, in-between, well-composed, but not necessarily self-dual.

3.6 Determining f_1 for self-dual local interpolation methods

Let us begin with the study of f_1, i.e., the function setting the values at the centers of the subdivided edges. This function has to be self-dual, symmetrical, and in-between, that's why we choose one of the most common function satisfying these constraints : the mean operator, i.e., $f_1 : \mathbb{R}^2 \mapsto \mathbb{R} : (v_1, v_2) \mapsto f_1(v_1, v_2) = (v_1 + v_2)/2$ (and then we avoided computational approximations by using only values in $2^n\mathbb{Z}$ for the original image u).

We will point out that there exists some other functions satisfying all these constraints (as $(a, b) \mapsto \mathrm{med}(a, b, 0)$) but we are not interested in these other cases for our applications, the mean operator seeming the most natural choice for our applications.

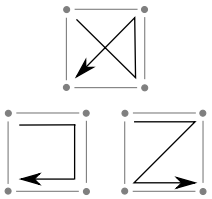

Fig. 7. The 3 possible configurations in 2D (modulo reflections and rotations).

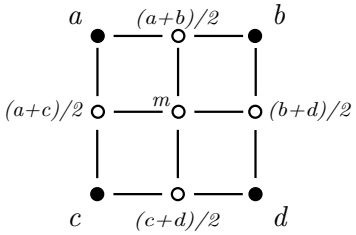

Fig. 8. $u'\big|_{\mathcal{G}(z)}$ for $z \in \mathbb{E}_2$ for any self-dual local interpolation after the application of f_1 (with m any value $\in \mathbb{R}$).

3.7 Equations of f_2 for self-dual local interpolation methods

Concerning f_2, i.e., the function which sets the values of u' at the centers of the subdivided faces, let us compute $I_0(u, z)$ and $I_{WC}(u, z)$ for any given $z \in \mathbb{E}_2$ to deduce $I_{sol}(u, z)$. Their values depend on what we call the *configurations* of $u\big|_{\mathbb{A}(z)}$.

Let us assume that $u\big|_{\mathbb{A}(z)} = \begin{pmatrix} a & b \\ c & d \end{pmatrix}$. Then a total of $4! = 24$ increasing orders are possible for these 4 values. Modulo reflections and axial symmetries, we obtain a total of 3 possible configurations: the *α-configurations* correspond to the relation $a \leq d < b \leq c$, the *U-configurations* to $a \leq b \leq d \leq c$, and the *Z-configurations* to $a \leq b \leq c \leq d$ (see Figure 7).

Lemma 4 *Let z be a point in $\mathbb{E}_2$. Modulo reflections and symmetries, an α-configuration implies that $u\big|_{\mathbb{A}(z)}$ is not well-composed, whereas a U- or Z-configuration implies that $u\big|_{\mathbb{A}(z)}$ is well-composed.*

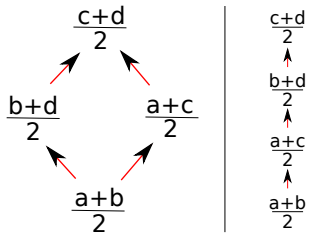

Fig. 9. The Hasse diagrams for the α- and the U-configurations (left) and for the Z-configuration (right).

Let us begin with the computation of $I_0(u, z)$ for any given $z \in \mathbb{E}_2$. From the values already set in u' on $\mathbb{P}(z) \subseteq \mathbb{E}_1$ by f_1 during the recursive process (see

Figure 8), we can compute $I_0(u,z)$ using the Hasse diagram (a mathematical diagram used to represent finite partially ordered sets with the biggest elements at the top) for each configuration (see Figure 9). We will obtain finally that $I_0(u,z) = \text{intvl}(\frac{a+c}{2}, \frac{b+d}{2})$ for the three configurations, with one important property: the median value of $u\big|_{\mathbb{A}(z)}$ always belongs to $I_0(u,z)$.

Let us follow with the computation of $I_{WC}(u,z)$, where $u'\big|_{\mathcal{G}(z)}$ (see Figure 8) has to satisfy four conditions:

$$\text{intvl}(a,m) \cap \text{intvl}((a+b)/2,(a+c)/2) \neq \emptyset \quad (1)$$
$$\text{intvl}((a+b)/2,(b+d)/2) \cap \text{intvl}(m,b) \neq \emptyset \quad (2)$$
$$\text{intvl}((a+c)/2,(c+d)/2) \cap \text{intvl}(m,c) \neq \emptyset \quad (3)$$
$$\text{intvl}(m,d) \cap \text{intvl}((c+d)/2,(b+d)/2) \neq \emptyset. \quad (4)$$

In the case of the α-configuration, (2) $\Rightarrow m \leq \frac{b+d}{2}$ and (4) $\Rightarrow m \geq \frac{b+d}{2}$, what implies $m = \frac{b+d}{2}$ and satisfies (1) and (3) in the same time. Consequently, $I_{WC}(u,z) = \{\text{med}\{u\big|_{\mathbb{A}(z)}\}\}$, and because $I_{WC}(u,z) \subseteq I_0(u,z)$, $I_{sol}(u,z) = \{\text{med}\{u\big|_{\mathbb{A}(z)}\}$ in the not well-composed case.

In the cases of the U- and the Z-configurations, we obtain that $I_{WC}(u,z) = [\frac{a+b}{2}, \frac{c+d}{2}] \supseteq I_0(u,z)$, so we conclude that $I_{sol}(u,z) = I_0(u,z)$.

Theorem 3 *Given an image $u : \mathcal{D} \mapsto \mathbb{R}$, any local interpolation method $\mathfrak{I}_{f_1,f_2,f_3}$ that satisfies $\mathcal{P}$ is such that $\forall\, z \in s(\mathcal{D}) \cap \mathbb{E}_2$:*

$$\begin{array}{ll} f_2(u\big|_{\mathbb{A}(z)}) = \text{med}\{u\big|_{\mathbb{A}(z)}\} & \text{if } u\big|_{\mathbb{A}(z)} \text{ is not W.C.,} \\ f_2(u\big|_{\mathbb{A}(z)}) \in I_0(u,z) & \text{otherwise.} \end{array}$$

Let z be a point in $s(\mathcal{D}) \cap \mathbb{E}_2$. Among the applications f_2 satisfying $\mathcal{P}$, there exists (at least) the *median method*, consisting in setting the value of $u'(z)$ at $\text{med}\{u\big|_{\mathbb{A}(z)}\}$ (in this case f_2 is an operator and not only a function), the *mean/median method of Latecki* [6] consisting in setting the value $u'(z)$ at $\text{mean}\{u\big|_{\mathbb{A}(z)}\}$ in the well-composed case and to $\text{med}\{u\big|_{\mathbb{A}(z)}\}$ otherwise, and also the *min/max method*, consisting in setting the value $u'(z)$ at $\frac{1}{2}(\min\{u\big|_{\mathbb{A}(z)}\} + \max\{u\big|_{\mathbb{A}(z)}\})$ in the well-composed case and to $\text{med}\{u\big|_{\mathbb{A}(z)}\}$ otherwise.

3.8 Equations of f_3 for local self-dual interpolation methods

Theorem 4 *No local interpolation method satisfying $\mathcal{P}$ makes well-composed images for $n \geq 3$ with one subdivision.*

Proof : Let z be the center of a subdivided cube. We have $u'\big|_{\mathbb{A}(z)}$ as in the Figure 10 (on the left). We apply the first interpolating function f_1 satisfying $\mathcal{P}$, i.e., we set the values of u' at the centers of the subdivided edges at the mean of the values on the vertices. Then we apply the second interpolating function f_2,

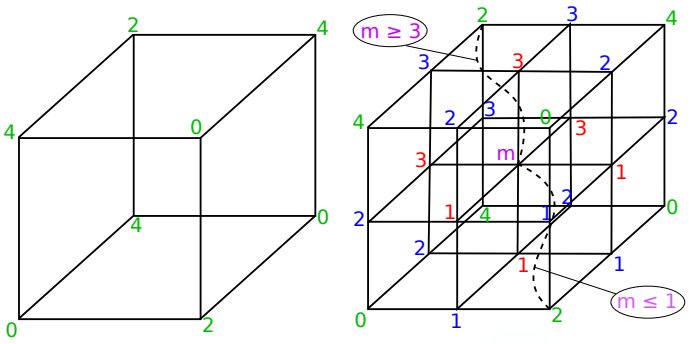

Fig. 10. A counter-example proving that any local interpolation method satisfying $\mathcal{P}$ with one subdivision cannot ensure well-composedness (the values of u' on $\mathbb{E}_0$ are in green, the ones on $\mathbb{E}_1$ are in blue, the ones on $\mathbb{E}_2$ are in red, and the ones on $\mathbb{E}_3$ are in purple).

which fixes the values of u' at the centers of the subdivided faces at the median of the values of u' at the four corresponding corners (because u is well-composed on none of the faces of the cube). Finally, referring to the properties that a function u' has to satisfy to be well-composed (see theorem 1), f_3 must satisfy in the same time the constraints $c \geq 3$ and $c \leq 1$ (both are the constraints of type 2) that are incompatible. So, no local interpolation method with one subdivision can satisfy the set of constraints $\mathcal{P}$ as soon as $n \geq 3$.

4 Conclusion

We have presented a characterization of well-composedness for 3D gray-valued images. We have also proved that an only scheme is possible for local interpolation methods, and that it implies that no local interpolation method satisfying $\mathcal{P}$ with one subdivision is able to make 3D well-composed images as soon as we choose the mean operator as interpolation method in 1D.

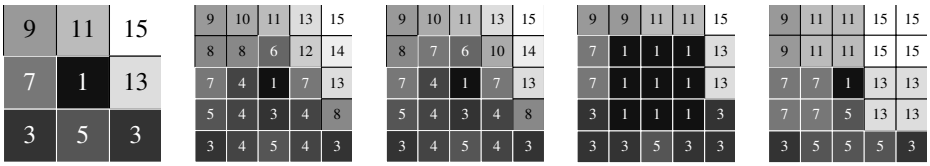

Fig. 11. From left to right: an image, then the interpolation results with the *median*, the *mean/median*, the *min* and the *max* methods respectively.

The different interpolation methods exposed in this paper, along with some other ones, are illustrated in Figure 11. The test image contains two α-, one U- and one Z- configurations.

We observe that the results of the *median* and the *mean/median* methods seem to be smoother than the others, while the *max* method overemphasizes bright components at the expense of the dark ones and the *min* method overemphasizes the dark components at the expense of the bright ones. However the min/max methods work in nD while the two other methods fail since $n \geq 3$ as it has been proven before.

Finally, two approaches for the future seem important to be tested. The first is to use an alternative to f_1 such as $\text{med}(a, b, 0)$ with a local interpolation method as exposed before. The secund, and it is our most promising results for the moment, is to use a non-local approach (as a front propagation algorithm), so we do not have to use any systematic operator f_1 anymore, neither to use an ordered interpolation method.

References

1. Caselles, V., Monasse, P.: Geometric Description of Images as Topographic Maps, Lecture Notes in Mathematics, vol. 1984. Springer-Verlag (2009)
2. Géraud, T.: Self-duality and discrete topology: Links between the morphological tree of shapes and well-composed gray-level images. Journée du Groupe de Travail de Géométrie Discrète (June 2013), `http://jgeodis2013.sciencesconf.org/conference/jgeodis2013/program/JGTGeoDis2013Geraud.pdf`
3. Géraud, T., Carlinet, E., Crozet, S., Najman, L.: A quasi-linear algorithm to compute the tree of shapes of n-D images. In: Hendriks, C.L., Borgefors, G., Strand, R. (eds.) Mathematical Morphology and Its Application to Signal and Image Processing – Proceedings of the 11th International Symposium on Mathematical Morphology (ISMM). Lecture Notes in Computer Science Series, vol. 7883, pp. 98–110. Springer, Heidelberg (2013)
4. Latecki, L.: 3D well-composed pictures. Graphical Models and Image Processing 59(3), 164–172 (May 1997)
5. Latecki, L., Eckhardt, U., Rosenfeld, A.: Well-composed sets. Computer Vision and Image Understanding 61(1), 70–83 (January 1995)
6. Latecki, L.J.: Well-composed sets. In: Advances in Imaging and Electron Physics. vol. 112, pp. 95–163. Academic Press (2000)
7. Marchadier, J., Arquès, D., Michelin, S.: Thinning grayscale well-composed images. Pattern Recognition Letters 25, 581–590 (April 2004)
8. Najman, L., Géraud, T.: Discrete set-valued continuity and interpolation. In: Hendriks, C.L., Borgefors, G., Strand, R. (eds.) Mathematical Morphology and Its Application to Signal and Image Processing – Proceedings of the 11th International Symposium on Mathematical Morphology (ISMM). Lecture Notes in Computer Science Series, vol. 7883, pp. 37–48. Springer, Heidelberg (2013)
9. Ngo, P., Passat, N., Kenmochi, Y., Talbot, H.: Topology-preserving rigid transformation of 2d digital images. IEEE Transactions on Image Processing 23(2), 885–897 (February 2014)
10. Rosenfeld, A.: Connectivity in digital pictures. Journal of the ACM 17(1), 146–160 (January 1970)